Journal of Photochemistry and Photobiology A: Chemistry 222 (2011) 185–191

Contents lists available at ScienceDirect

Journal of Photochemistry and Photobiology A: Chemistry

journal homepage: www.elsevier.com/locate/jphotochem

Synthesis, characterization and introduction of a new ion-coordinating ruthenium sensitizer dye in quasi-solid state TiO_2 solar cells

Ryan C. White[a], João E. Benedetti[a], Agnaldo D. Gonçalves[a], Wanderson Romão[b], Boniek G. Vaz[b], Marcos N. Eberlin[b], Carlos R.D. Correia[c], Marco A. De Paoli[a], Ana F. Nogueira[a,*]

[a] Laboratory of Nanotechnology and Solar Energy, Institute of Chemistry, University of Campinas – UNICAMP, P.O. Box 6154, 13083-970, Campinas, SP, Brazil
[b] ThoMSon Mass Spectrometry Laboratory, Institute of Chemistry, University of Campinas – UNICAMP, 13083-970, Campinas, SP, Brazil
[c] Laboratory for the Synthesis of Organic Substances, Institute of Chemistry, University of Campinas – UNICAMP, 13083-970, Campinas, SP, Brazil

ARTICLE INFO

Article history:
Received 9 December 2010
Received in revised form 20 May 2011
Accepted 29 May 2011
Available online 12 June 2011

Keywords:
Ion-coordinating dye
Heteroleptic sensitizer
Gel polymer electrolyte
Quasi-solid state solar cells

ABSTRACT

A new ion-coordinating heteroleptic ruthenium(II) dye was synthesized by attaching two crown ether moieties in the 4,4′ positions of one of the bipyridine ligands. This new dye (named as RC730) was characterized by UV-Vis spectroscopy, CHN elemental analysis, NMR and electrospray ionization Fourier transform-ion cyclotron resonance mass spectrometry (ESI FT-ICR MS). In order to investigate the properties of these ion-coordinating species, dye-sensitized solar cells were assembled with a gel polymer electrolyte based on two different cations: lithium and sodium. The devices were characterized by *J–V* curves under 100 mW cm^{-2}, incident photon to current conversion efficiency spectra (IPCE) and photovoltage decay transients under open-circuit conditions. The solar cells based on the new heteroleptic dye provided higher photocurrent and photovoltage when lithium was used in the electrolyte instead of sodium cations, reaching overall conversion efficiencies up to 2%. This behavior might be related to the ability of the ion-coordinating RC730 dye to trap Li ions, minimizing the conduction band edge shift. When the polymer electrolyte based on lithium is used, the IPCE spectra show a maximum efficiency of 31% at the maximum absorption peak of the RC730 dye (ca. 530 nm).

1. Introduction

Since their inception 19 years ago, dye-sensitized solar cells (DSCs) have emerged as a viable alternative to inorganic silicon-based solar cells [1]. Their low cost of production and high efficiency of energy conversion, recently reaching more than 11% [2], make such devices promising alternatives for the generation of new, inexpensive solar cells [3].

DSCs are made up of two major chemical components: a sensitizer dye (responsible for light absorption and generation of charge carriers) and an electrolyte that serves as a shuttle between the two electrodes and is responsible for dye regeneration. To date, highly absorptive, relatively stable and well-tested dyes consist of ruthenium polypyridyl complexes anchored to a porous metal oxide electrode such as TiO_2 nanoparticulated films [4]. The most efficient electrolytes are liquid substances that allow for the rapid diffusion of ions from the counter-electrode to the oxidized dye complex [5,6]. Whereas liquids are the optimum medium to facilitate ion flow, there are some inherent drawbacks when incorporating them into DSCs. For instance, electrolyte leakage, evaporation, corrosion and difficulty of large scale production all cause substantial problems when bringing DSCs to market [5]. Many efforts have been made to overcome these challenges, for example, by replacing the liquid electrolyte by room temperature ionic liquids [7,8], hole transport materials [9–12] or polymer and gel electrolytes [13–20].

Over the past 14 years, our laboratory has focused on novel types of electrolytes for DSCs in the form of solid-state polymer electrolytes based on copolymers of poly(ethylene oxide) (PEO) [19,20,21] and two recent reviews on these efforts have appeared [19,21]. Although the quasi-solid nature of this polymeric material is a great advantage because it reduces the problems mentioned above, it also has the effect of slowing down ionic diffusion, thereby reducing the efficiency of the solar cell. With the intent of improving ionic mobility, we have recently incorporated lithium coordinating 12-crown-4 ether into our gel electrolyte formulation [22]. The results showed an overall increase in solar cell efficiency due to two factors: (a) an increased open-circuit voltage (V_{oc}) due to the coordination of Li^+ ions by the crown ether [23] and (b) effective shielding from the porous metal oxide layer. The other benefit was increased short-circuit current (I_{sc}) as a consequence of decreased Li^+ mobility, whereas increased iodide mobility was observed [22,24]. To further analyze the effect of the crown-ether

* Corresponding author. Tel.: +55 19 3521 3029; fax: +55 19 3521 3023.
E-mail address: anaflavia@iqm.unicamp.br (A.F. Nogueira).

1010-6030/$ – see front matter © 2011 Elsevier B.V. All rights reserved.
doi:10.1016/j.jphotochem.2011.05.020

moiety within the solar cell, we have designed a novel sensitizer complex with two crown-ethers covalently linked to the ruthenium complex itself.

The modification of the ruthenium complex discussed in this work was inspired by Grätzel and coworkers [25], who to improve solar cell efficiencies, have covalently modified ruthenium sensitizer dyes with different organic groups. One particular dye of note is the K51 dye in which the triethylene oxide methyl ether (TEOME) group was introduced on the 4,4′ position of a 2,2′-bipyridine ligand with ion-coordinating properties to capture the Li^+ ions [25]. Devices tested with K51 and a solid-state electrolyte showed a significant increase in the open-circuit voltage, when Li^+ was added into the electrolyte. Unfortunately, ethylene oxide chain ion-coordinating arm of the K51 dye increased its instability during accelerated aging tests due to the desorption of the bipyridine ligands. This effect was related to the hydrophilic nature of the ligand. To improve the stability of the DSCs using an ion-coordinating sensitizer, Grätzel and coworkers have also developed a more hydrophobic K68 dye [26]. This dye exhibited ion-coordinating properties, due to the presence of TEOME substituents, and also high hydrophobicity due to presence of heptyl chains at the end of the alkoxy chains. Therefore, the K68 dye presented more stability and less aggregation than K51. Fig. 1 shows the molecular structure of the heteroleptic RC730 dye. The molecular structures of the sensitizers K51 and N719 are also shown for comparison.

As may be seen in Fig. 1, RC730 dye has a cyclic ethylene oxide chain opposed to the open-chain ethylene oxide moieties in the K51 dye. Therefore, in this work we present the synthesis, characterization and introduction of a new ion-coordinating ruthenium sensitizer (named as RC730, Fig. 1) in quasi-solid state solar cells assembled with gel polymer electrolyte based on poly(ethylene oxide-co-2-(2-methoxyethoxy) ethyl glycidylether) (P(EO/EM), γ-butyrolactone (GBL), iodine and two different salts (LiI or NaI).

2. Experimental

2.1. RC730 synthesis

Synthesis of the 4,4′-bis(12-crown-4 methylether)-2,2′ bipyridine ligand (**1**).

A THF solution (3 mL) of 2-hydroxymethyl 12-crown-4 ether (0.160 g, 0.78 mmol) was combined with NaH (20.5 mg, 0.85 mmol) and stirred under argon for 1 h. A THF solution (2 mL) of 4,4′-bis(chloromethyl)-2,2′-bipyridine, Cl_2Bpy, prepared as described previously [27] (98.2 mg, 0.38 mmol) was then added and the mixture was stirred for 4 h at room temperature, until thin layer chromatography (TLC) showed total consumption of the starting material. The solution was taken up into CH_2Cl_2 (50 mL) and washed with water (3 mL × 50 mL) and evaporated under reduced pressure to an orange-yellow oil. The oil was purified on a silica-gel column (pre-treated with 10% triethylamine in hexane) to yield a clear yellow oil: 0.108 mg (48%); ^{1}H NMR ($CDCl_3$, 500 MHz) δ 3.57–3.91 (m, 30H), 4.66 (s, 4H), 7.34 (d, J = 5.0 Hz, 2H), 8.32 (s, 2H), 8.64 (d, J = 5.0 Hz, 2H); ^{13}C NMR ($CDCl_3$, 125 MHz) 70.2, 70.3, 70.6, 70.6, 70.7, 70.9, 71.0, 71.5, 71.8, 78.6, 119.2, 121.8, 148.6, 149.2, 156.0.

Synthesis of the (tetrabutylammonium)$_2$ Ru(4,4′-biscarboxylate-2,2′bipyridine)(4,4′-bis[12-crown-4 methylether] -2,2′bipyridine)(NCS)$_2$ (RC730).

$RuCl_2$(p-cymene) (21.0 mg, 0.034 mmol) and 1 (41.0 mg, 0.069 mmol) were dissolved in 5 mL of DMF. The reaction mixture was heated to 60 °C under argon for 4 h with constant stirring. Subsequently, 4,4′-dicarboxylic acid-2,2′-bipyridine (17.0 mg, 0.070 mmol) was added to the reaction flask and the reaction mixture was refluxed at 140 °C for 4 h. Finally, an excess of KNCS was added to the mixture and reflux continued for another 4 h. The reaction mixture was cooled to room temperature and the solvent was removed under vacuum. Water was added to the flask, and the dark purple solid was collected by suction filtration, washed with water and diethyl ether and then dried under vacuum. This crude product was then dissolved in a methanolic solution of tetrabutylammonium hydroxide and purified by passing the compound three times through a Sephadex LH-20 column with methanol as the eluent to afford 61.0 mg (60%) of the pure complex salt. ^{1}H NMR ($CDOD_3$, 500 MHz) δ 1.00 (t, 3H), 1.40 (h, 16H), 1.66 (p, 16H), 3.23 (t, 16H), 3.50–4.17 (m, 34H), 4.59 (s, 4H), 7.10 (d, 1H), 7.57 (dd, 2H), 7.67 (d, 1H), 7.74 (d, 1H), 8.29 (d, 1H), 8.34 (s, 1H), 8.50 (s, 1H), 8.83 (s, 1H), 9.00 (s, 1H), 9.36 (s, 1H), 9.50 (s, 1H). CHN Analytical calculation for $C_{76}H_{122}N_8O_{14}RuS_2$: C, 59.4; H, 8.0; N, 7.3%; found: C: 60.1; H, 8.3; N, 7.7%. Molar mass of the RC730 dye = 1536.8 g mol^{-1}.

2.2. Electrospray ionization Fourier transform-ion cyclotron resonance mass spectrometry (ESI FT-ICR MS)

To study the constituents of the dye, a variety of analytical techniques have been used. ESI FT-ICR MS offers ultra-high mass resolving power ($m/\Delta m_{50\%}$ is the mass spectral peak full width at half-maximum peak height) and can be useful to resolve and characterize many components present in our dye molecule [28,29].

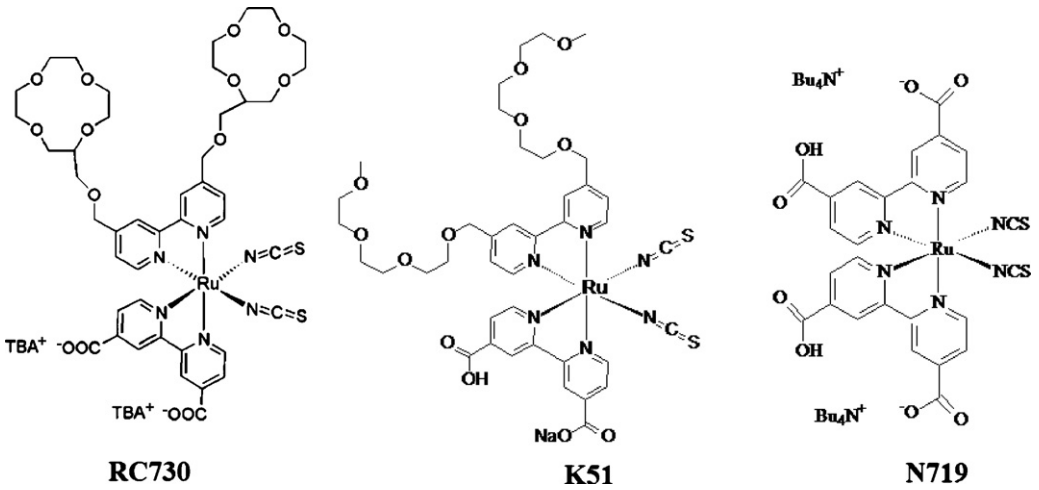

Fig. 1. Molecular structures of sensitizers RC730, K51 and N719.

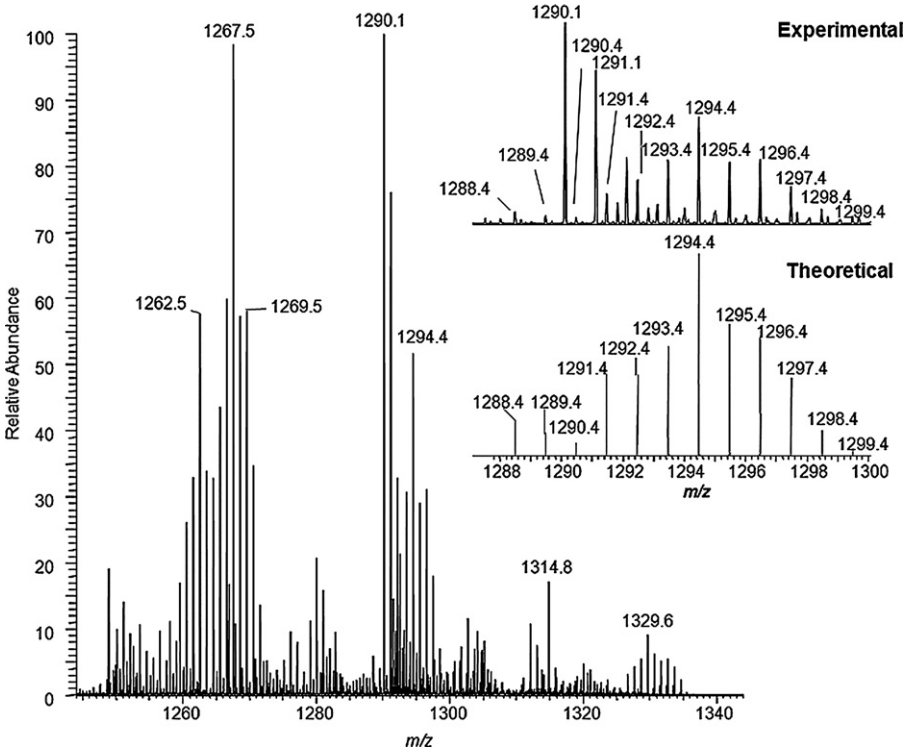

Fig. 2. ESI(−) FT-ICR MS for a methanolic solution of the new heteroleptic ruthenium dye RC730.

This technique was successfully used earlier for characterizing other supramolecular ruthenium based complexes [30–33].

For characterization by ESI FT-ICR, the RC730 dye was dissolved in 1 mL of methanol. For ESI in the negative ion mode, 2 μL of an aqueous solution of 1% ammonium hydroxide was added to the solution and electrosprayed with an automated chip-based nano-ESI-MS Triversa NanoMate 100 system (Advion BioSciences, Ithaca, NY, USA). The analyte solution was loaded into 96-well plates (total volume of 100 μL in each well) and analyzed by a 7 T LTQ FT Ultra mass spectrometer (ThermoScientific, Bremen, Germany). ESI(−) general conditions were: gas pressure of 0.3 psi, capillary voltage of 1.55 kV and solution flow rate of 250 $\mu L\,min^{-1}$. Mass spectra were acquired by summing up 100 microscans and processed using the Xcalibur 2.0 software (ThermoScientific, Bremen, Germany).

2.3. UV-Vis spectroscopy

The UV–Vis spectra were measured in a 1-cm path length quartz cell using a Hewlett Packard 8453 spectrophotometer for two dyes: N719, known as [*cis*-*bis*(isothiocyanate) *bis*(2,2′-bipyridyl-4,4′-dicarboxylate) ruthenium(II)] (*bis*-tetrabutylammonium) and RC730. Both dyes were dissolved separately in anhydrous ethanol.

2.4. Preparation of the gel electrolyte

The copolymer poly(ethylene oxide-co-2-(2-methoxyethoxy) ethyl glycidyl ether) P(EO-EM) was used as received from Daiso Co. Ltd. (Osaka, Japan) and had a molar mass of $1 \times 10^6\,g\,mol^{-1}$, according to the supplier. The electrolyte samples were prepared by the dissolution of the copolymer, γ-butyrolactone (GBL), iodine and the salt in acetone (all chemicals used were from Aldrich, 99%, except the copolymer). Two electrolytes were prepared, using LiI or NaI. Both electrolytes were prepared by using the same P(EO-EM):GLB ratio, that is, 0.1:0.9 (wt%). The concentrations of salt and iodine were kept constant at 0.5 $mol\,L^{-1}$ and 0.05 $mol\,L^{-1}$, respectively. The electrolyte solutions were kept under constant stirring for 1 week before use.

2.5. Solar cell assembly and characterization

The dye-sensitized solar cells were assembled as follows: a TiO_2 suspension (Solaronix) was deposited by the doctor blading technique onto the transparent conducting oxide substrate (Hartford Glass Co. Inc., 8–12 Ω/□). Adhesive tape (Scotch®) was used as frame and spacer. The films were heated to 450 °C for 30 min, giving a layer of ∼8 μm thickness as measured with a Taylor Hobson, Form Talysurf series profilometer. The electrodes, at a temperature of ca. 80 °C, were then immersed in a $2.5 \times 10^{-4}\,mol\,L^{-1}$ solution of new dye RC730 in anhydrous ethanol and maintained for ca. 14 h at room temperature. For comparison, the electrodes were also immersed in a solution with the same concentration of the N719 dye in anhydrous ethanol for ca. 14 h at room temperature. Afterwards, the electrodes were washed with ethanol and dried in air. The gel polymer electrolyte deposition onto the sensitized TiO_2 films was carried out inside a vacuum chamber using the method described by Caruso and co-workers [34]. The average solar cell area was 0.25 cm^2. The *J*–*V* curves of the solar cells were measured under AM 1.5 illumination ($100\,mW\,cm^{-2}$) using a Xe (Hg) light source and filters. The polychromatic light intensity at the electrode position was measured with a Newport Optical Power Meter model 1830-C. The voltage decay measurements were carried out under open-circuit conditions by switching off the light and monitoring the open-circuit voltage (V_{oc}) decay in the dark for a given period of time [35,36]. The incident photon to current conversion efficiencies (IPCE) spectra of the solar cells were measured using a monochromator (Oriel) coupled to the optical bench described above.

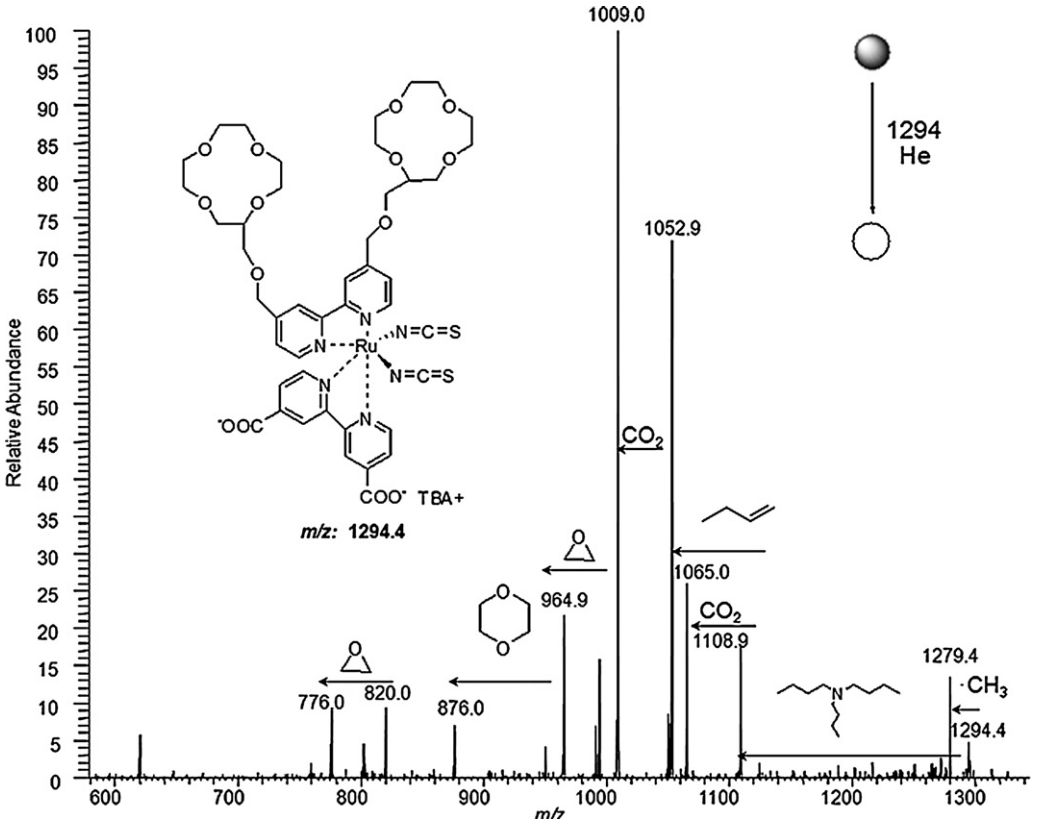

Fig. 3. ESI(−) FT-ICR MS/MS of the ion of *m*/*z* 1294.4.

3. Results and discussion

3.1. ESI FT-ICR MS

Fig. 2 shows the ESI(−) FT-ICR mass spectrum for a methanolic solution of the RC730 ruthenium dye. Note the detection of the dye as the $[M+TBA]^-$ anion of *m*/*z* 1294.4 (whereas M^{2-} is the doubly charged Ru-anion and TBA^+ is the counter cation) with the characteristic cluster of isotopologue ions. The experimental isotopologue pattern of the dye is quite diverse mainly due to the Ru, and closely matches the theoretical pattern as calculated by the Xcalibur 2.0 software (insets in Fig. 2). This match corroborates the proposed structure for the dye. The ions of *m*/*z* 1290.1 and *m*/*z* 1291.1 disturb the isotopologue distribution for the experimental spectrum but they are due to impurities, also detected in the ESI(−) FT-ICR MS of the starting reagent. The ions of *m*/*z* 1262.5 and *m*/*z* 1267.5 are due to ions with compositions (typical isotopologue distributions) similar to the dye anion $[M+TBA]^-$, therefore displaying subtle structure variations. The ion of *m*/*z* 1262.5 likely corresponds to the product of a nucleophylic substitution reaction that occurs due to the presence of traces of water where the two NCS Ru ligands are hydrolyzed to NCO. The ion of *m*/*z* 1267.5 corresponds to replacement of one of the NCS ligands by CH_3OH.

Fig. 3 shows the ESI(−) FT-ICR MS/MS for the ion of *m*/*z* 1294.4. The dissociation chemistry observed is also in agreement with the proposed structure for RC730. The fragment ions of *m*/*z* 1279.4 and 1109.0 are formed due to losses of $CH_3^{\bullet}$ and a neutral N-(*n*But)$_3$ amine molecule from the TBA counter cation. The fragment ions of *m*/*z* 1065.0 and *m*/*z* 1052.9 are likely formed via neutral losses of CO_2 (44 Da) and $CH_3CH_2CH{=}CH_2$ (56 Da) from the ion of *m*/*z* 1108.9. Subsequently, the ion of *m*/*z* 1052.9 loses CO_2 to produce the ion of *m*/*z* 1009.0. Both CO_2 eliminations originate from the carboxylic acid groups present in the bipyridine ligand. Other fragment ions such as those of *m*/*z* 964.9, 876.0 and 776.0 are formed via neutral losses of cyclic ethers from the crown ether group of the second bipyridine ligand.

3.2. UV–Vis spectra

Fig. 4 shows the UV–Vis electronic absorption spectra of the new heteroleptic Ru dye (RC730, solid line) and N719 (dashed line), both in absolute ethanol.

The absorption spectrum of the N719 complex shows two broad visible bands at 534 and 390 nm, resulting from MLCT (metal-to-ligand charge-transfer transitions) [37,38]. The band at

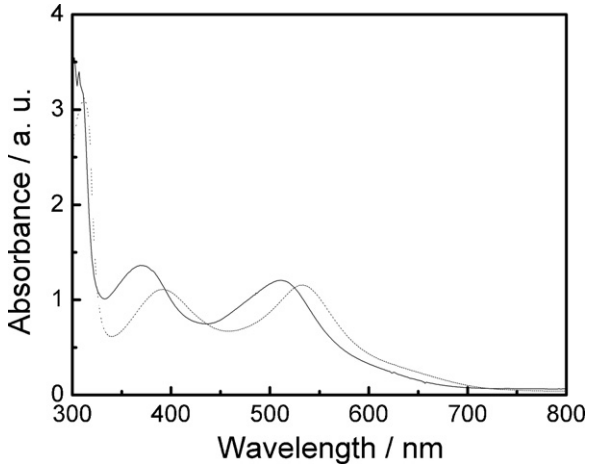

Fig. 4. UV–Vis spectra of the N719 dye (dashed line) and the new heteroleptic Ru dye (solid line) in ethanol.

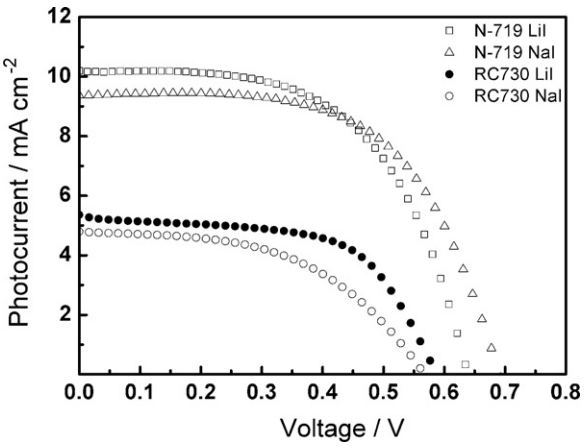

Fig. 5. *J–V* curves of DSC based on the N719 dye and the new heteroleptic Ru dye synthesized in this work (RC730). The gel polymer electrolytes were composed of P(EO/EM)/GBL/salt/I2 (salt = LiI or NaI). The measurements were carried out under 100 mW cm^{-2} and the average DSC area was 0.25 cm^2. The *J–V* curves represent the average behavior for at least 3 devices.

310 nm results from intraligand (π–π*) transitions. The spectrum for RC730, a blue shift is observed for both UV and visible absorption bands, which might be is associated to the electron withdrawing effect from the crown ether moieties.

3.3. DSC characterization

Fig. 5 shows the photocurrent density–voltage (*J–V*) curves of the dye-sensitized solar cells based on the N719 dye and the new heteroleptic Ru dye with Na and Li-based polymer gel electrolytes (Table 1).

Dye-sensitized solar cells based on the N719 dye provided higher photocurrent densities for both Na and Li-based gel polymer electrolytes, almost twice those values measured for the DSCs based on the new heteroleptic Ru dye. Higher open-circuit voltage values were also observed for the DSCs based on the N719 dye for both Na and Li-based polymer electrolytes compared to the analogous DSCs based on the new heteroleptic Ru dye. We will focus our discussion initially on the standard (N719) dye.

The difference in V_{oc} values among the DSCs assembled with the gel polymer electrolyte prepared with different salts (LiI or NaI) is associated with the interfacial energetics of dye-sensitized TiO_2 films and the electrolyte. This effect has been investigated by Fitzmaurice and co-workers [39,40]. After electron injection into the conduction band of TiO_2 from the excited state of the dye, the cations adsorb onto the surface of the TiO_2 nanoparticles or intercalate into the TiO_2 lattice for charge compensation [41]. The potential drop in the Helmholtz layer depends on adsorbed salt cations. Consequently, the different size of the cations will give rise to a different potential for the conduction band edge of the nanocrystalline TiO_2 films, shifting the potential more negatively (according to the vacuum scale) as the cation radius decreases [39,42,43]. The same effect was also observed by Bhattacharya et al. [44] for quasi-solid state solar cells employing gel polymer electrolytes. The V_{oc} is therefore enhanced with the increase in cation radius (from Li^+ to Na^+). When the conduction band shifts negatively, however, the driving force for the injection of electrons from the dye excited state into the conduction band of TiO_2 also increases, leading to higher injection efficiency. This effect can explain the improvement in photocurrent observed for the DSCs assembled with the gel polymer electrolyte based on the lithium salt.

The initial idea in the present work was to trap the lithium ions (but not sodium ions) from the electrolyte composition by using coordinating species in the dye structure in order to inhibit their adsorption onto the TiO_2 nanoparticle surface, since the adsorption of lithium ions onto the TiO_2 surface has been shown to decrease the V_{oc} due to the conduction band edge (E_{cb}) shifting to more negative values [40,41,45]. This behavior could be circumvented by trapping the Li^+ ions in the dye structure. This way the V_{oc} would not be impaired by the deleterious effect of Li^+ adsorption. It has also been shown that 4-*tert*-butyl-pyridine (TBP) may improve V_{oc} significantly with a small decrease in J_{sc} [46]. When lithium is dissolved in the electrolyte, the effect of TBP in improving the V_{oc} has recently been associated with the suppression of the specific adsorption of Li^+ through the formation of a complex with the TBP molecule, retarding the downward shift of the conduction band edge [47].

The higher photocurrent density values observed for DSCs based on the N719 dye compared to the new heteroleptic Ru dye prepared in this work may be explained based on several factors, such as dye structure, dye geometry on the TiO_2 surface, and the ambipolar diffusion model [45].

The dye structure plays a decisive role on the absorption, charge transfer and regeneration kinetics. The lower V_{oc} values from the DSCs based on the new heteroleptic Ru dye synthesized in this work, compared to the analogous N719-based DSCs, are in excellent agreement with the literature [48]. In the present work there are two different dyes: a homoleptic dye (N719) and a heteroleptic dye (RC730). Homoleptic dyes have two equivalent bipyridine ligands, whereas heteroleptic dyes were designed to enhance the performance and/or long-term stability of DSCs by functionalizing one of the bipyridine ligands. Unfortunately, the V_{oc} from DSCs based on heteroleptic dyes are significantly smaller than those observed for DSCs based on homoleptic dyes with the same number of protons [48]. The difference between homoleptic and heteroleptic dyes has been associated with their adsorption modes onto the TiO_2 surface since heteroleptic dyes adsorb onto the TiO_2 surface necessarily via carboxylic groups residing on the same bipyridine ligand [48]. The different adsorption mode of the dye also influences the position of the TiO_2 conduction band due to the direction of the dipole moment, as has been recently computed for homoleptic and heteroleptic dyes [48]. The lower V_{oc} values observed for DSCs based on the heteroleptic RC730 dye in this work, compared to the analogous DSCs based on the N719 dye, might therefore be also associated to the adsorption mode of the RC730 dye onto the TiO_2 surface.

The ambipolar diffusion model has recently been applied to explain the behavior of charge transport in DSCs [45]. Within this framework, the measured diffusion coefficients are associated with the diffusion coefficients and concentration of negative and positive charges. For a large difference between the concentration of positive and negative charges, the measured diffusion coefficient will reflect the diffusion of minority carriers (electrons or holes), depending on the cation concentration and electron density [45]. The electrons injected from the excited state of the dye into the conduction band of TiO_2 will therefore be screened by the cations in the electrolyte composition. Since no net electrical field is present, the charge carriers will move by diffusion rather than drift.

In the present work, the dye structure containing the crown-ether ligands might trap Li ions from the electrolyte. The cation concentration in the electrolyte will therefore be smaller to some

Table 1
Electrical parameters of the dye-sensitized solar cells based on the N719 dye and the new heteroleptic Ru dye (RC730). The ionic conductivity of the electrolytes is also displayed.

Dye	Salt	σ (S cm^{-1})	V_{oc}(V)	J_{sc} (mA cm^{-2})	FF	η (%)
(N719)	LiI	3.0×10^{-3}	0.64	10.2	0.57	3.72
	NaI	2.8×10^{-3}	0.69	9.45	0.58	3.78
(RC730)	LiI	3.0×10^{-3}	0.58	5.35	0.60	1.87
	NaI	2.8×10^{-3}	0.56	4.79	0.51	1.37

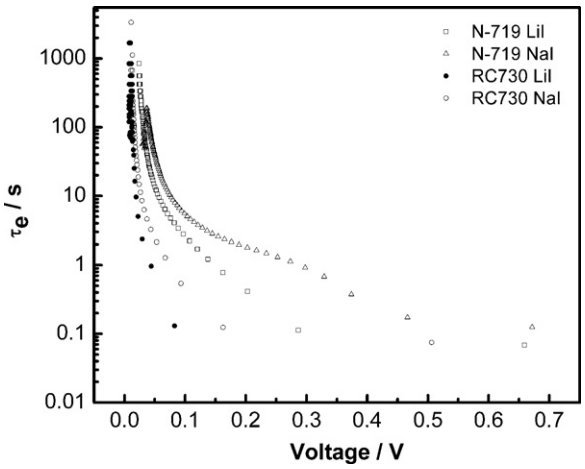

Fig. 6. Open-circuit voltage decay transients of the DSCs based on the N719 and the new Ru dye prepared in this work. The gel polymer electrolytes were composed of LiI or NaI.

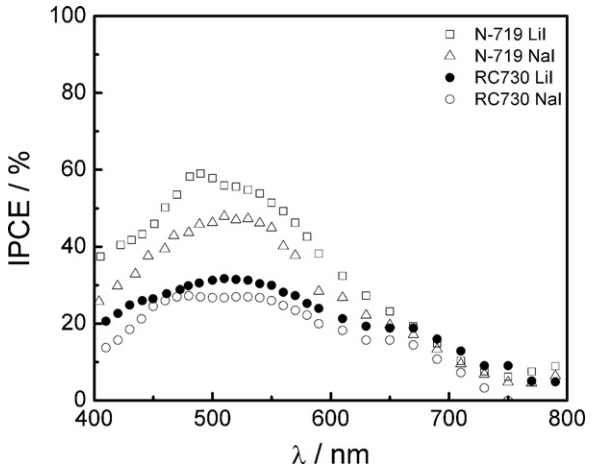

Fig. 7. Incident photon to current conversion efficiency (IPCE) spectra of the DSCs based on the N719 and the new Ru dye prepared in this work. The gel polymer electrolyte was composed of LiI or NaI.

extent and the remaining non-trapped Li^+ and the other cations in the electrolyte are used to screen the charge arising from the photoinjected electrons. The less efficient electron screening on the TiO_2 nanoparticle surface arising from the smaller cation concentration in the electrolyte promotes higher recombination losses, which can help to explain the smaller V_{oc} and J_{sc} values observed for the DSCs based on the synthesized dye in this work compared to the DSCs based on the N719 dye. However, the effect of trapping lithium ions in the dye structure may also increase the recombination losses if the trapped species are located near the TiO_2 surface. This effect cannot be ruled out when considering the recombination losses in this work. It is likely that increasing the amount of Li^+ ions trapped in the dye structure, near the TiO_2 surface, might make the diffusion of negative charges of the redox shuttle more difficult due to electrostatic interaction. Therefore, higher recombination losses might take place, which can help explain the lower photocurrent and voltage in DSCs based on the RC730 dye compared to the analogous DSCs based on the N719 dye.

For the solar cells based on the new heteroleptic dye, the DSCs with Li^+ ions in the electrolyte composition provided higher J_{sc} and V_{oc} values compared to the DSCs based on the same dye and Na^+ in the electrolyte. The higher V_{oc} for the former might provide some evidence for the Li-trapping ability of the crown ether moieties from the new heteroleptic Ru dye, since some Li^+ ions would not be able to absorb to the TiO_2 surface, minimizing the conduction band edge shift.

The calculated charge lifetimes under open-circuit conditions (Fig. 6) are in excellent agreement with the *J–V* curves.

The higher lifetime from the DSCs based on the N719 dye using the gel polymer electrolyte composed of NaI corroborates the higher V_{oc} values compared to the analogous DSCs based on the polymer electrolyte with LiI. The lower performances from the DSCs based on the RC730 dye, both with NaI or LiI, are in excellent agreement with the smaller charge lifetimes compared to the analogous DSCs based on the N719 dye. This behavior confirms that recombination losses are of major importance in our work and arise from the use of the new heteroleptic dye in DSC. The strong coordination of the small cations close to the TiO_2 surface, has turned the interface processes more active.

The incident photon to current conversion efficiency (IPCE) spectra of the DSCs based on the N719 and the new Ru dye are shown in Fig. 7. The action spectra of the new heteroleptic Ru dye synthesized in this work reflect the lower performance discussed before, that is, the maximum IPCE at 530 nm is almost two times higher for the N719 dye compared to the new heteroleptic Ru dye prepared in this work. The maximum IPCE values at 530 nm for the DSCs based on the N719 dye were 55% (Li-based polymer electrolyte) and 47% (Na-based polymer electrolyte), while for the RC730 dye the values were 31% (Li-based polymer electrolyte) and 27% (Na-based polymer electrolyte).

4. Conclusion

A new heteroleptic Ru dye (RC730) containing crown-ether moities on 4,4′ positions of the bipyridine ligand was successfully synthesized, as confirmed by ESI(−) FT-ICR MS analysis. DSCs were assembled using two different types of gel electrolytes (with NaI or LiI) and the N719 dye was used for comparison. The higher photocurrent density values observed for DSCs based on the N719, dye compared to the new heteroleptic Ru dye prepared in this work, can be explained by a different dye structure (homoleptic versus heteroleptic), dye geometry on the TiO_2 surface, the decrease of available cations for charge compensation and increased local accumulation of electron accepting species. We believe that all these factors are important here and the fact that all contribute to increase recombination make them difficult to separate. Our results indicate that when replacing the liquid electrolyte by a gel polymer electrolyte, the processes occurring at the interfaces became extremely sensitive to local environment and recombination is further accelerate. A small positive effect on V_{oc} was observed with our dye when lithium was used in the electrolyte instead of sodium cations. This means that removing part of Li^+ cations may be interesting, but trapping them strongly is not effective. The results presented here are important for future design of dyes to be applied in quasi-solid DSSC.

Acknowledgements

The authors acknowledge FAPESP (fellowships 06/58998-3 and 08/51001-9), Renami, CNPq and National Science Foundation (USA) for financial support, Daiso Co. Ltd., Osaka (Japan) for kindly providing the copolymer and Prof. Carol H. Collins for English revision. We also acknowledge the LMF/LNLS (National Synchrotron Light Laboratory, Campinas, SP, Brazil) for providing the platinized counter-electrodes

References

[1] B. ÓRegan, M. Grätzel, A low-cost, high-efficiency solar cell based on dye-sensitized colloidal TiO_2 films, Nature 353 (1991) 737–740.

[2] M Grätzel, Les nouvelles cellules solaires nanocritallines, Actual. Chim. 308–309 (2007) 57–60.
[3] M. Grätzel, Recent advances in sensitized mesoscopic solar cells, Acc. Chem. Res. 42 (2009) 1788–1798.
[4] D. Kuang, S. Ito, B. Wenger, C. Klein, J.E. Moser, R. Humphry-Baker, S.M. Zakeeruddin, M. Grätzel, High molar extinction coefficient heteroleptic ruthenium complexes for thin film dye-sensitized solar cells, J. Am. Chem. Soc. 128 (2006) 4146–4154.
[5] J. Wu, Z. Lan, S. Hao, P. Li, J. Lin, M. Huang, L. Fang, Y. Huang, Progress on the electrolytes for dye-sensitized solar cells, Pure Appl. Chem. 80 (2008) 2241–2258.
[6] J.H. Wu, S.C. Hao, Z. Lan, J.M. Lin, M.L. Huang, Y.F. Huang, L.Q. Fang, S. Yin, T. Sato, A thermoplastic gel electrolyte for stable quasi-solid-state dye-sensitized solar cells, Adv. Funct. Mater. 17 (2007) 2645–2652.
[7] P. Wang, S.M. Zakeeruddin, J.E. Moser, R. Humphry-Baker, M. Grätzel, A solvent-free, $SeCN^-/(SeCN)_3^-$ based ionic liquid electrolyte for high-efficiency dye-sensitized nanocrystalline solar cells, J. Am. Chem. Soc. 126 (2004) 7164–7165.
[8] S. Ito, S.M. Zakeeruddin, P. Comte, P. Liska, D. Kuang, M. Grätzel, Bifacial dye-sensitized solar cells based on an ionic liquid electrolyte, Nat. Photonics 2 (2008) 693–698.
[9] J. Bandara, H. Weerasinghe, Solid-state dye-sensitized solar cell with p-type NiO as a hole collector, Sol. Energy Mater. Sol. Cells 85 (2005) 385–390.
[10] J.C. Fatuch, M.A. Soto-Oviedo, C.O. Avellaneda, M.F. Franco, W. Romão, M.A. De Paoli, A.F. Nogueira, Synthesis and characterization of aniline copolymers containing carboxylic groups and their application as sensitizer and hole conductor in solar cells, Synth. Met. 159 (2009) 2348–2354.
[11] G.K.R. Senadeera, T. Kitamura, Y. Wada, S. Yanagida, Enhanced photoresponses of polypyrrole on surface modified TiO_2 with self-assembled monolayers, J. Photochem. Photobiol. A 184 (2006) 234–239.
[12] J.E. Kroeze, N. Hirata, L. Schmidt-Mende, C. Orizu, S.D. Ogier, K. Carr, M. Grätzel, J.R. Durrant, Parameters influencing charge separation in solid-state dye-sensitized solar cells using novel hole conductors, Adv. Funct. Mater. 16 (2006) 1832–1838.
[13] A.F. Nogueira, J.R. Durrant, M.A. De Paoli, Dye-sensitized nanocrystalline solar cells employing a polymer electrolyte, Adv. Mater. 13 (2001) 826–830.
[14] T. Kato, A. Okazaki, S. Hayase, Latent gel electrolyte precursors for quasi-solid dye sensitized solar cells: the comparison of nano-particle cross-linkers with polymer cross-linkers, J. Photochem. Photobiol. A 179 (2006) 42–48.
[15] J.E. Benedetti, A.D. Gonçalves, A.L.B. Formiga, M.A. De Paoli, X. Li, J.R. Durrant, A.F. Nogueira, A polymer gel electrolyte composed of a poly(ethylene oxide) copolymer and the influence of its composition on the dynamics and performance of dye-sensitized solar cells, J. Power Sources 195 (2010) 1246–1255.
[16] F.S. Freitas, J.N. Freitas, B.I. Ito, M.A. De Paoli, A.F. Nogueira, Electrochemical and structural characterization of polymer gel electrolytes based on a PEO copolymer and an imidazolium-based ionic liquid for dye-sensitized solar cells, ACS Appl. Mater. Interfaces 1 (2009) 2870–2877.
[17] J.N. Freitas, C. Longo, A.F. Nogueira, M.A. De Paoli, Solar module using dye-sensitized solar cells with a polymer electrolyte, Sol. Energy Mater. Sol. Cells 92 (2008) 1110–1114.
[18] J.H. Wu, Z. Lan, J.M. Lin, M.L. Huang, S.C. Hao, T. Sato, S. Yin, A novel thermosetting gel electrolyte for stable quasi-solid-state dye-sensitized solar cells, Adv. Mater. 19 (2007) 4006–4011.
[19] J.N. Freitas, A.F. Nogueira, M.A. De Paoli, New insights into dye-sensitized solar cells with polymer electrolytes, J. Mater. Chem. 19 (2009) 5279–5294.
[20] A.F. Nogueira, N. Alonso-Vante, M.A. De Paoli, Solid-state photoelectrochemical device using poly(o-methoxy aniline) as sensitizer and an ionic conductive elastomer as electrolyte, Synth. Met. 105 (1999) 23–27.
[21] A.F. Nogueira, C. Longo, M.A. De Paoli, Polymers in dye sensitized solar cells: overview and perspectives, Coord. Chem. Rev. 248 (2004) 1455–1468.
[22] J.E. Benedetti, M.A. De Paoli, A.F. Nogueira, Enhancement of photocurrent generation and open circuit voltage in dye-sensitized solar cells using Li^+ trapping species in the gel electrolyte, Chem. Commun. 9 (2008) 1121–1123.
[23] K.C. Huang, R. Vittal, K.C. Ho, Effects of crown ethers in nanocomposite silica-gel electrolytes on the performance of quasi-solid-state dye-sensitized solar cells, Sol. Energy Mater. Sol. Cells 94 (2010) 675–679.
[24] C. Shi, S. Dai, K. Wang, X. Pan, L. Zeng, L. Hu, F. Kong, Li Guo, Influence of various cations onredox behavior of I^- and I_3^- and comparison between KI complex with 18-crown-6 and 1,2-dimethyl-3-propylimidazolium iodide in dye-sensitized solar cells, Electrochim. Acta 50 (2005) 2597–2602.
[25] D. Kuang, C. Klein, H.J. Snaith, J.-E. Moser, R. Humphry-Baker, P. Comte, S.M. Zakeeruddin, M. Grätzel, Ion coordinating sensitizer for high efficiency mesoscopic dye-sensitized solar cells: influence of lithium ions on the photovoltaic performance of liquid and solid-state cells, Nano Lett. 6 (2006) 769–773.
[26] D. Kuang, C. Klein, H.J. Snaith, R. Humphry-Baker, S.M. Zakeeruddin, M. Grätzel, A new ion-coordinating ruthenium sensitizer for mesoscopic dye-sensitized solar cells, Inorg. Chim. Acta 361 (2008) 699–706.
[27] C.L. Fraser, N.R. Anastasi, J.J.S. Lamba, Synthesis of halomethyl and other bipyridine derivatives by reaction of 4, 4′-bis[(trimethylsilyl)methyl]-2,2′-bipyridine with electrophiles in the presence of fluoride ion, J. Org. Chem. 62 (1997) 9314–9317.
[28] M.B. Comisarow, A.G. Marshall, Frequency-sweep Fourier transform ion cyclotron resonance spectroscopy, Chem. Phys. Lett. 26 (1974) 489–490.
[29] A.G. Marshall, Accurate mass measurement: taking full advantage of nature's isotopic complexity, Phys. B 346–347 (2004) 503–508.
[30] D.M. Tomazela, F.C. Gozzo, I. Mayer, F.M. Engelmann, K. Araki, H.E. Toma, M.N. Eberlin, Electrospray mass and tandem mass spectrometry of homologous and isomeric singly, doubly, triply and quadruply charged cationic ruthenated meso-(phenyl)m-(meta- and para-pyridyl)n (m + n = 4) macrocyclic porphyrin complexes, J. Mass Spectrom. 39 (2004) 1161–1167.
[31] I. Mayer, M.N. Eberlin, D.M. Tomazela, H.E. Toma, K. Araki, Supramolecular conformational effects in the electrocatalytic properties of electrostatic assembled films of meso(3- and 4-pyridyl) isomers of tetraruthenated porphyrins, J. Braz. Chem. Soc. 16 (2005) 418–425.
[32] I. Mayer, A.L.B. Formiga, F.M. Engelmann, H. Winnischofer, P.V. Oliveira, D.M. Tomazela, M.N. Eberlin, H.E. Toma, K. Araki, Study of the spectroscopic and electrochemical properties of tetraruthenated porphyrins by theoretical–experimental approach, Inorg. Chim. Acta 358 (2005) 2629–2642.
[33] M.N. Eberlin, D.M. Tomazela, K. Araki, A.D.P. Alexiou, A.L.B. Formiga, H.E. Toma, S. Nikolaou, Electrospray ionization tandem mass spectrometry of polymetallic μ-oxo- and carboxylate-bridged $[Ru_3O(CH_3COO)_6(Py)_2(L)]^+$ complexes: intrinsic ligand (L) affinities with direct access to steric effects, Organomettalics 25 (2006) 3245–3250.
[34] H. Han, U. Bach, Y.B. Cheng, R.A. Caruso, Increased nanopore filling: effect on monolithic all-solid-state dye-sensitized solar cells, Appl. Phys. Lett. 90 (2007) 213510.
[35] M. Quintana, T. Edvinsson, A. Hagfeldt, G. Boschloo, Comparison of dye-sensitized ZnO and TiO_2 solar cells: studies of charge transport and carrier lifetime, J. Phys. Chem. C 111 (2007) 1035–1041.
[36] A. Zaban, M. Greenshtein, J. Bisquert, Determination of the electron lifetime in nanocrystalline dye solar cells by open-circuit voltage decay measurements, Chem. Phys. Chem. 4 (2003) 859–864.
[37] M.K. Nazeeruddin, A. Kay, I. Rodicio, R. Humphry-Baker, E. Mueller, P. Liska, N. Vlachopoulos, M. Grätzel, Conversion of light to electricity by cis-X_2bis(2,2′-bipyridyl-4,4′-dicarboxylate)ruthenium(II) charge-transfer sensitizers (X = Cl^-, Br^-, I^-, CN^- and SCN^-) on nanocrystalline titanium dioxide electrodes, J. Am. Chem. Soc. 115 (1993) 6382–6390.
[38] M.K. Nazeeruddin, D. Di Censo, R. Humphry-Baker, M. Grätzel, Highly selective and reversible optical, colorimetric, and electrochemical detection of mercury(II) by amphiphilic ruthenium complexes anchored onto mesoporous oxide films, Adv. Funct. Mater. 16 (2006) 189–194.
[39] G. Redmond, D. Fitzmaurice, Spectroscopic determination of flatband potentials for polycrystalline titania electrodes in nonaqueous solvents, J. Phys. Chem. 97 (1993) 1426–1430.
[40] B. Enright, G. Redmond, D. Fitzmaurice, Spectroscopic determination of flatband potentials for polycrystalline TiO_2 electrodes in mixed solvent systems, J. Phys. Chem. 98 (1994) 6195–6200.
[41] Y. Liu, A. Hagfeldt, X.R. Xiao, S.E. Lindquist, Investigation of influence of redox species on the interfacial energetics of a dye-sensitized nanoporous TiO_2 solar cell, Sol. Energy Mater. Sol. Cells 55 (1998) 267–281.
[42] L.A. Lyon, J.T. Hupp, Energetics of semiconductor electrode/solution interfaces: EQCM evidence for charge-compensating cation adsorption and intercalation during accumulation layer formation in the titanium dioxide/acetonitrile system, J. Phys. Chem. 99 (1995) 15718–15720.
[43] B.I. Lemon, J.T. Hupp, Electrochemical quartz crystal microbalance studies of electron addition at nanocrystalline tin oxide/water and zinc oxide/water interfaces: evidence for band-edge-determining proton uptake, J. Phys. Chem. B 101 (1997) 2426–2429.
[44] B. Bhattacharya, J.Y. Lee, J. Geng, H.T. Jung, J.K. Park, Effect of cation size on solid polymer electrolyte based dye-sensitized solar cells, Langmuir 25 (2009) 3276–3281.
[45] N. Kopidakis, E.A. Schiff, N.-G. Park, J. van de Lagemaat, A.J. Frank, Ambipolar diffusion of photocarriers in electrolyte-filled, nanoporous TiO_2, J. Phys. Chem. B 104 (2000) 3930–3936.
[46] S.Y. Huang, G. Schlichthörl, A.J. Nozik, M. Grätzel, A.J. Frank, Charge recombination in dye-sensitized nanocrystalline TiO_2 solar cells, J. Phys. Chem. B 101 (1997) 2576–2582.
[47] S. Nakade, T. Kanzaki, W. Kubo, T. Kitamura, Y. Wada, S. Yanagida, Role of electrolytes on charge recombination in dye-sensitized TiO_2 solar cell (1): the case of solar cells using the I^-/I_3^- redox couple, J. Phys. Chem. B 109 (2005) 3480–3487.
[48] F. De Angelis, S. Fantacci, A. Selloni, M. Grätzel, M.K. Nazeeruddin, Influence of the sensitizer adsorption mode on the open-circuit potential of dye-sensitized solar cells, Nano Lett. 7 (2007) 3189–3195.